Electron spins at surface, interface and vacancy detected by spin-polarized positron annihilation spectroscopy

Journal of Physics: Conference Series **3029** (2025) 012021 doi:10.1088/1742-6596/3029/1/012021

Electron spins at surface, interface and vacancy detected by spin-polarized positron annihilation spectroscopy

A. Kawasuso[1*], M. Maekawa[1], S. Li[1], Y. Du[1], S. Sakai[1], N. Kanazawa[2]

[1] National Institute for Quantum Science and Technology, 1233, Watanuki, Takasaki, Gunma, 370-1292, Japan
[2] Institute of Industrial Science, The University of Tokyo, 4-6-1 Komaba Meguro-ku, Tokyo, 153-8505, Japan

[*]E-mail: kawasuso.atsuo@qst.go.jp

Abstract. We have been developing spin-polarized positron annihilation spectroscopy for applications of spintronics materials. In this article, we report how electron spins at surface, interface and vacancy are detected in spintronics materials, with examples of clean ferromagnets, MgO/FeSi(B20) and Mn_2FeGa.

1. Introduction

Energy saving of electronic devices is an urgent issue because of rapid increase in energy consumption in information and communication technology. In addition to this, current device technology has one more problem, i.e., plateau of performance. To settle these matters, the so-called spintronics research field has emerged in the last decades [1]. New concepts and principles found in fundamental solid-state physics, such as the novel spin phenomena occurring at the surface and interface [2] and the discovery of a new class of topological materials [3, 4] would be the foundation of technological innovation. Today, vast materials and phenomena related to spin generation, manipulation, and transport are extensively studied in an interdisciplinary field [5].

To understand unprecedented phenomena related to electron spins in materials, new experimental tools should be established. It is thought that spin-polarized positron annihilation spectroscopy (SP-PAS) may provide the unique opportunity meeting the above requirement. As a matter of fact, this method started to be used for studying ferromagnetic band structures already in 1950's upon the discovery of the parity violation in the weak interaction. After an incubation, one breakthrough, spin-polarized surface positronium spectroscopy, was demonstrated by the Michigan group in 1982 [6]. A decade ago, we started to utilize SP-PAS to follow up vital spintronics field. In this paper, we show how electron spins at surface, interface and vacancy in spintronics materials are detected taking examples of ferromagnetic surfaces, MgO/FeSi(B20) and Mn_2FeGa.

2. Electron spins detected by SP-PAS

2.1 Surface spins

Spin polarization of surface electrons can be determined by "spin-polarized surface positronium spectroscopy" measuring the intensity of spin-triplet positronium, which is formed from positrons and surface electrons and emitted into vacuum, upon reversal of relative direction of

positron and electron spins. The details of analysis are summarized elsewhere [7-9]. As compared to conventional photoemission spectroscopy, this method has a marked advantage that the spin polarization of top-most surface layer can be determined thanks to the fact that positronium is formed only at the vacuum side of outermost surface except for some special cases.

Table 1 lists the spin polarizations obtained for Fe, Co and Ni surfaces by spin-polarized surface positronium spectroscopy without energy discrimination of positronium in an ultra-high vacuum condition (base pressure of 10^{-8} Pa). These metal surfaces all exhibit positive spin polarizations. This result is consistent with the original work by the Michigan group for Ni(110) surface [6]. On the other hand, it is theoretically predicted that, just below the Fermi levels, the spin polarizations of these ferromagnets are exclusively negative, i.e., minority electrons are predominant [10]. The above discrepancy in sign may be explained by considering participation of electrons in positronium formation not only around the Fermi level, but also in the occupied states below it. From the energy conservation, positrons may pick up electrons located from the Fermi level to the depth of positronium formation potential, Φ_{Ps}. To examine this assumption roughly, we calculated electron-positron density of states (e-p DOS) at surface, which is defined by an overlap integral of positron density and position-dependent electron DOS [7,8]. Figure 1 shows e-p DOS calculated for Fe, Co and Ni surfaces. By further integrating e-p DOS from Φ_{Ps} (calculated to be −3.55 eV for Fe, −3.58 eV for Co and −3.2 eV for Ni in a similar manner in Refs. [11-13]) to the Fermi level, we obtained the spin polarizations being observed by positrons to be +22 % for Fe(001), +6% for Co(0001) and +0.4% for Ni(111) as listed in Table 1. Thus, the positive sign and the tendency of magnitudes of spin polarization in experiment may be explained by the above-mentioned consideration. The significantly lower spin polarization for Fe in experiment as compared to calculation is probably due to the degradation of Fe surface during measurement (typically it takes a few hours) even in ultra-high vacuum condition. To minimize such a discrepancy, it may be important to shorten measurement time with a stronger positron beam and also in further higher vacuum condition, i.e., below 10^{-8} Pa. The above method was further

Table 1. Spin-polarizations for Fe, Co and Ni surfaces with different crystal planes obtained by spin-polarized surface positronium spectroscopy (Experiment) and calculated values from surface electron-positron density of states (Calculation).

Fe	Co	Ni
	Experiment	
+4(1) %, (001)	+2.1(9) %, (001)	+0.4(4) %, (001)
	+4.3(9) %, (0001)	+1.4(3) %, (111)
	Calculation	
+22 %, (001)	+6 %, (0001)	+0.4 %, (111)

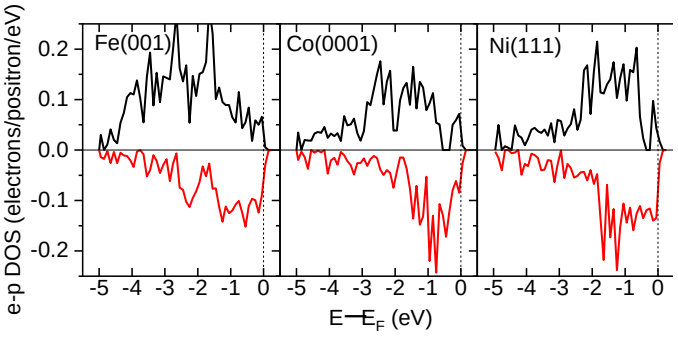

Figure 1. Electron-positron surface density of states (e-p DOS) calculated for Fe(001), Co(0001) and Ni(111) surfaces. Positive and negative axes represent majority and minority spin states, respectively.

successfully applied to the observation of magnetic proximity effect on graphene formed on ferromagnets [7,8]. It was found that graphene tightly bound on the surface of ferromagnet is effectively spin-polarized, while loosely bound graphene mainly through van der Waals force is not, suggesting importance of hybridization between graphene and the surface of ferromagnet. Although the above scenario may be naturally accepted and hence nothing non-trivial, an important point is again that such information is not accessible with conventional methods [14].

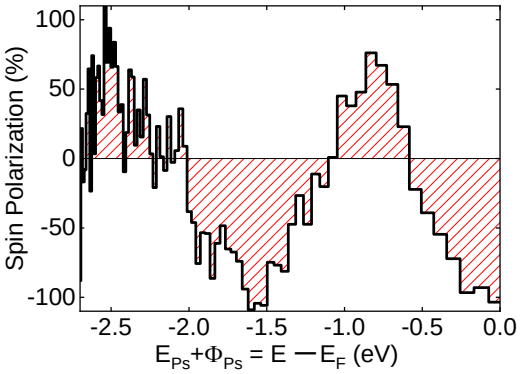

Figure 2. Surface electron spin polarization obtained by spin-polarized positronium time-of-flight spectroscopy for Ni(111) surface.

Simple surface positronium spectroscopy without energy discrimination of positronium provides only average spin polarization of occupied electrons participating in positronium formation. To determine spin polarization as a function of electron energy level, especially just around the Fermi level, the energy spectroscopy of positronium is essential. For this purpose, the positronium time-of-flight method was developed with an electrostatic beam system, which can maintain positron spin polarization during beam transportation [15]. The energy resolution was improved by inserting a positronium quencher at the position of lead slit through which annihilation gamma rays are detected [16]. Figure 2 shows the spin polarization of Ni(111) surface determined by this method. Negative spin polarization just below the Fermi level is now clearly seen. This spectrum may be quantitatively reproduced by the e-p DOS shown in Fig. 1 after convolution with the detailed energy-dependent resolution function as reported elsewhere [15].

2.2 Interface-confined spins ~MgO/FeSi~

The Doppler broadening of annihilation radiation (DBAR) spectrum may change upon reversal of mutual spin direction of positrons and electrons. We call this method as magnetic Doppler broadening (MDB) spectroscopy. Also, the difference of DBAR spectra obtained under positive and negative magnetic fields is called MDB spectrum. Here, the sign of field is defined as parallel/antiparallel field to the positron spin polarization. Actually, this property was well confirmed for conventional bulk ferromagnets, i.e., Fe, Co, Ni and Gd [17,18]. Spin polarization confined at buried interface may be similarly detected by tuning incident positron energy appropriately.

Here, as an example, FeSi is picked up. FeSi is known as a paramagnetic material exhibiting metal-insulator transition at low temperatures and giant magnetic susceptibility above room temperature that are similar to the feature of Kondo insulator [19]. A recent study shows the appearance of novel spin texture on the Fe-terminated surface of FeSi caused by the strong spin-orbit coupling and the nearly quantized Zak phase [20]. Furthermore, such ferromagnetic atomic layer can be effectively confined by capping the surface with MgO, BaF_2 or CaF_2 layers [21]. While the confined spins at the interface have been observed using polarized neutron reflectometry under an in-plane magnetic field, direct observation at zero field is desirable to further support evidence of the spontaneous ferromagnetic ordering and its perpendicular magnetic anisotropy.

Figure 3(a) shows the MDB intensity obtained for MgO/FeSi under remanent condition as a function of incident positron energy. That is, magnetic field (1 T) was applied to out-of-plane direction for a few seconds and subsequently longitudinally spin-polarized positrons were

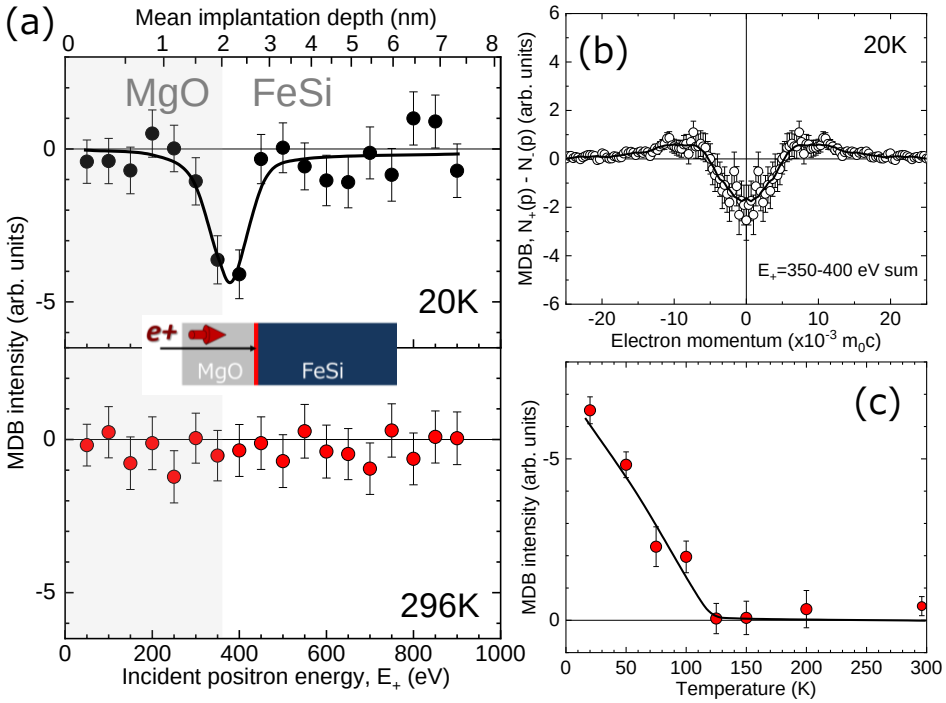

Figure 3. (a) MDB intensity as a function of incident positron energy (E_+) at 20 K and 296 K. Mean implantation depth is shown in the upper horizontal axis. Solid line is an eye guide. (b) MDB spectrum obtained at 20 K. Data for E_+=350 eV and 400eV are summed. (c) Temperature dependence of MDB intensity at E_+=400 eV. Solid line is an eye guide.

implanted. At room temperature, the MDB intensity is almost null, while at 20 K, it shows a change just at the incident energy (E_+=350-400 eV) corresponding to the MgO/FeSi interface together with the MDB spectrum in Fig. 3(b). Figure 3(c) shows the temperature dependence of MDB intensity. It disappears above 120 K, suggesting that the Curie temperature of the confined ferromagnetic layer is well below room temperature. The above results are consistent with the previous report on the emergence of confined ferromagnetic moments at the interface between FeSi and MgO [20].

2.3 Local spins at vacancy ~Mn_2FeGa~

MDB spectroscopy described in the preceding subsection may also be applied to the detection of local spins at atomic vacancies. Actually, several studies have been carried out on the issues of vacancy-induced ferromagnetism in ZnO [22] and GaN [23], and of anomalous Hall conduction of Weyl semimetals [24]. It seems that there are no competitive methods against MDB spectroscopy as for the detection of local spins at atomic vacancies regardless of metals and non-metals.

Here, as an example, ferrimagnetic cubic Mn_2FeGa is introduced. This material is an inverse Heusler alloy and a candidate material for optically-driven magnetic memory device. The basic concept is that ferrimagnetically coupled electron spins at Mn atoms are easily flipped by short pulse laser illumination, which is called all optical magnetization switching (AOS). Previous work demonstrated that metastable cubic Mn_2FeGa, which may exhibit both ferrimagnetic and half-metallic characteristics and hence well suited for AOS device applications, can be epitaxially grown on Cr buffer layer on MgO substrate [25]. However, in the characterisation of material quality, the inclusion of defects has not been examined.

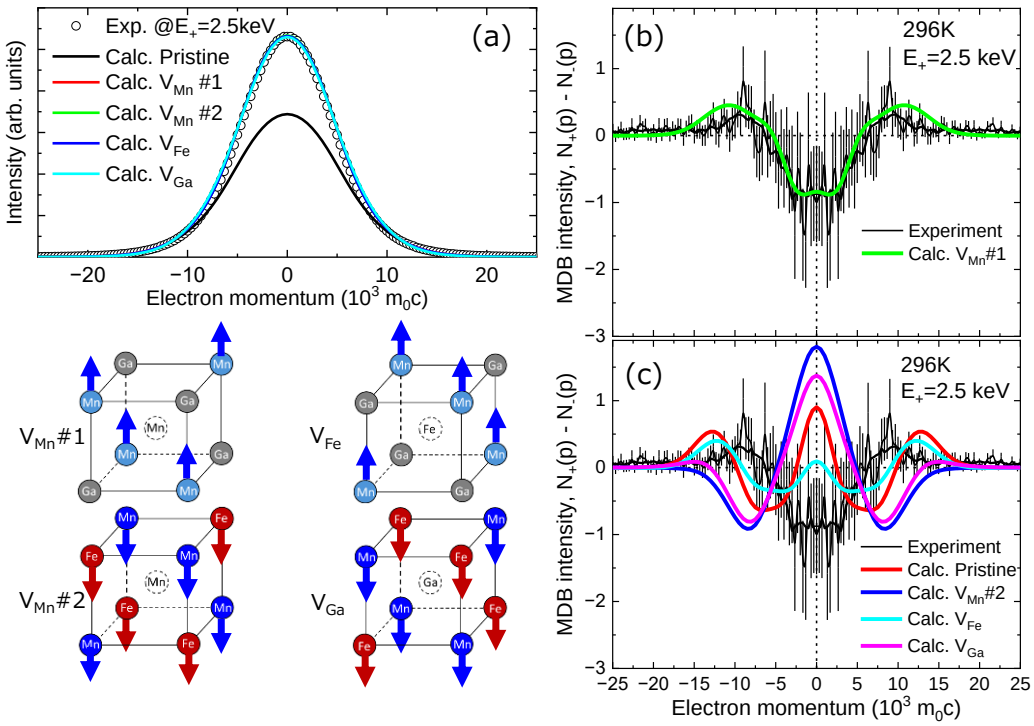

Figure 4. (a) Conventional DBAR spectrum obtained for the Mn_2FeGa layer at incident positron energy of E_+=2.5 keV. Solid lines are calculated DBAR spectra for pristine crystal and four different single vacancies schematically shown below the figure. These four types of vacancies give almost the same curve shapes in this scale and hence they are not distinguishable. (b) MDB spectrum obtained for the Mn_2FeGa layer (E_+=2.5 keV) and comparison with calculation for Mn vacancy surrounded by Mn and Ga atoms (V_{Mn} #1). (c) Same as (b) but with calculations for pristine Mn_2FeGa, Mn vacancy surrounded by Mn and Fe atoms (V_{Mn} #2), Fe vacancy and Ga vacancy.

Figure 4(a) shows conventional DBAR spectrum obtained for 50 nm thick Mn_2FeGa epitaxial film on 2 nm thick Cr on MgO(001) substrate with a capping layer of 5 nm thick AlO_x at the incident positron energy of E_+=2.5 keV. Calculated DBAR spectra for pristine and four kinds of single vacancies are also drawn. From the comparison between experiment and calculation, it is found that the present Mn_2FeGa contains a copious amount of vacancies, probably single vacancies. However, it is rather problematic to determine which of four kinds of single vacancies are major species from the above comparison. Figures 4(b) and 4(c) show the magnetic DBAR spectrum and the comparison with calculation. It is found that experiment is most well explained by one of Mn vacancies surrounded by Mn and Ga atoms (V_{Mn} #1). Since AOS occurs due to the ferrimagnetically coupled electron spins on Mn atoms, for improving its efficiency, it might be important to find some means to reduce Mn vacancies.

3. Summary

In this paper, some applications of spin-polarized positron annihilation spectroscopy to spintronics materials focusing on surface, interface and vacancy were introduced. Different kinds of materials and phenomena appear next to next in spintronics research field. In this respect, the role of spin-polarized positron annihilation spectroscopy must be substantial. The present

method runs with ^{22}Na source. Spontaneous spin polarization of positrons from β-decay radioisotopes is a gift. However, there is a technical limitation of intensity. For further progress, early establishment of highly spin-polarized intense positron beam facility is waited for.

4. Acknowledgement

This work was financially supported by JSPS KAKENHI Grant-in-Aid for Scientific Research (S) (No. JP23H05462), (B) (No. JP21H03748), and JST, CREST Grant Number JPMJCR23O3.

References

[1] J. Puebla, J. Kim, K. Kondou, Y. Otani, Commun. Mater. **1**, 24 (2020).
[2] F. Hellman et al., Rev. Mod. Phys. **89**, 025006 (2017).
[3] Y. Ando, J. Phys. Soc. Jpn. **82**, 102001 (2013).
[4] N.P. Armitage, E.J. Mele, A. Vishwanath, Rev. Mod. Phys. **90**, 015001(2018).
[5] A. Hirohata et al., J. Magn. Magn. Mater., **509**, 166711 (2020).
[6] D. W. Gidley, A. R. Koymen, T. W. Capehart, Phys. Rev. Lett. **49**, 1779(1982).
[7] A. Miyashita, M. Maekawa, K. Wada, A. Kawasuso, T. Watanabe, S. Entani, and S. Sakai, Phys. Rev. B **97**, 195405 (2018).
[8] A. Miyashita, S. Li, S. Sakai, M. Maekawa, and A. Kawasuso, Phys. Rev. B **102**, 045425 (2020).
[9] H. Li, M. Maekawa, A. Miyashita, A. Kawasuso, Defect and Diffusion Forum **373**, 65 (2017).
[10] A. J. Freeman, C. L. Fu, S. Ohnishi and M. Weinert, "Electronic and Magnetic Structure of Solid Surfaces: Chapter 1 of Part I", in "Polarized Electrons in Surface Physics", Ed. R. Feder, World Scientific, 1985.
[11] A. Kawasuso, K. Wada, A. Miyashita, M. Maekawa, H. Iwamori, S. Iida, and Y. Nagashima et al., J. Phys.: Condens. Matter **33**, 035006 (2021).
[12] A. Kawasuso, M. Maekawa, A. Miyashita , K. Wada, Y. Nagashima and A. Ishida, J. Phys. B: At. Mol. Opt. Phys. **54**, 205202(2021).
[13] A. Kawasuso, M. Maekawa, A. Miyashita, and K. Wada, T. Kaiwa and Y. Nagashima, Phys. Rev. B **97**, 245303 (2018).
[14] S. J. Gilbert, P. A. Dowben, J. Phys. D: Appl. Phys. **53**, 343001 (2020).
[15] M. Maekawa, A. Miyashita S. Sakai , S. L , S. Entani , and A. Kawasuso, and Y. Sakuraba, Phys. Rev. Lett. **126**, 186401 (2021).
[16] A. Kawasuso and M. Maekawa Acta Phys. Polo. B Proc. Suppl., 17, 1-A4(2024).
[17] A. Kawasuso, M. Maekawa, Y. Fukaya, A. Yabuuchi, and I. Mochizuki, Phys. Rev. B **83**, 100406(R) (2011).
[18] A. Kawasuso, M. Maekawa, Y. Fukaya, A. Yabuuchi, and I. Mochizuki, Phys. Rev. **85**, 024417 (2012).
[19] Z. Fisk, J. L. Sarrao, J. D. Thompson, D. Mandrus, M. F. Hundley, A. Miglori, B. Bucher, Z. Schlesinger, G. Aeppli, E. Bucher, J. F. DiTusa, C. S. Oglesby, H-R. Ott, P. C. Canfield, S. E. Brown, Physica B: Condensed Matter, 206–207, 798 (1995).
[20] Y. Ohtsuka, N. Kanazawa, M. Hirayama, A. Matsui, T. Nomoto, R. Arita, T. Nakajima, T. Hanashima, V. Ukleev, H. Aoki, M. Mogi, K. Fujiwara, A. Tsukazaki, M. Ichikawa, M. Kawasaki, Y. Tokura, Sci. Adv. **7**, eabj0498 (2021).
[21] T. Hori, N. Kanazawa, M. Hirayama, K. Fujiwara, A. Tsukazaki, M. Ichikawa, M. Kawasaki, Y. Tokura, Adv. Mater., **35**, 2206801 (2023).
[22] M. Maekawa, H. Abe, A. Miyashita, S. Sakai, S. Yamamoto, and A. Kawasuso, Appl. Phys. Lett., **110**, 172402(2017).
[23] M. Maekawa, A. Miyashita, S. Sakai, and A. Kawasuso, Phys. Rev. B **102**, 054427(2020).
[24] A. Miyashita, M. Maekawa, Y. Shimoyama, N. Seko, A. Kawasuso, and R. Y. Umetsu, J. Phys.: Condens. Matter **34**, 045701(2022).
[25] P. D. Bentley, S. Li, K. Masuda, Y. Miura, Y. Du, T. Mitsui, K. Fujiwara, Y. Kobayashi, T. Guo, G. Yu, C. Suzuki, S. Yamamoto, F. Zheng, Y. Sakuraba, and S. Sakai, Phys. Rev. Materials, **7**, 064404 (2023).